VISUALIZATION OF PARTICLE COMPLEXES IN THE PLASMA MEMBRANE OF *MICRASTERIAS DENTICULATA* ASSOCIATED WITH THE FORMATION OF CELLULOSE FIBRILS IN PRIMARY AND SECONDARY CELL WALLS

THOMAS H. GIDDINGS, JR., DANNY L. BROWER, and L. ANDREW STAEHELIN

From the Department of Molecular, Cellular and Developmental Biology, University of Colorado, Boulder, Colorado 80309. Dr. Brower's present address is the MRC Laboratory of Molecular Biology, Cambridge, CB-2 2QH England.

ABSTRACT

Highly ordered arrays of intramembrane particles are observed in freeze-fractured plasma membranes of the green alga *Micrasterias denticulata* during the synthesis of the secondary cell wall. The observable architecture of the complex consists primarily of a precise hexagonal array of from 3 to 175 rosettes, consisting of 6 particles each, which fracture with the P-face. The complexes are observed at the ends of impressions of cellulose fibrils. The distance between rows of rosettes is equal to the center-to-center distance between parallel cellulose fibrils of the secondary wall. Correlation of the structure of the complex with the pattern of deposition indicates that the size of a given fibril is proportional to the number of rosettes engaged in its formation. Vesicles containing hexagonal arrays of rosettes are found in the cytoplasm and can be observed in the process of fusing with the plasma membrane, suggesting that the complexes are first assembled in the cytoplasm and then incorporated into the plasma membrane, where they become active in fibril formation. Single rosettes appear to be responsible for the synthesis of microfibrils during primary wall growth. Similar rosettes have now been detected in a green alga, in fern protonemata, and in higher plant cells. This structure, therefore, probably represents a significant component of the cellulose synthesizing mechanism in a large variety of plant cells.

KEY WORDS cellulose synthesis · plasma membrane · intramembrane complexes · freeze-fracture · *Micrasterias*

The plasma membrane of plant cells is generally believed to play a significant role in the synthesis of linear β-1,4-glucan polymers and in the assembly of these chains into microfibrils of cellulose. Several investigators have employed the freeze-etch technique in an attempt to visualize specific intramembrane proteins or complexes involved in this process (2–5, 8, 14–19, 22–24, 26–30, 32). Much of this work is discussed in a recent review (3). Rows of particles called "terminal complexes" have been shown in association with the growing ends of microfibrils in the green alga *Oocystis* (2,

14, 24). Less distinctive, cylindrical terminal complexes have been reported in another alga, *Glaucocystis* (28). The terminal complex of *Acetobacter xylinum* consists of a linear array of particles located in the outer membrane (4, 31, 32). The distribution of these particles appears to coincide with that of pores visualized on etched outer surfaces (32), and it has been proposed that each particle (or pore) gives rise to a single microfibril. Microfibrils then associate to form the one large cellulose ribbon synthesized by each cell. Globular complexes in association with microfibril ends in corn root cells (15–17) and in elongating cotton fibers (27) have been described. In the case of corn root cells (15, 16), rosettes consisting of approximately six particles were found on the P-face of the plasma membrane at the tips of the impressions of underlying microfibrils. This finding is particularly intriguing in light of the results presented here.

In our study, we have investigated the architecture of the plasma membrane of *Micrasterias denticulata* during both primary and secondary wall synthesis. Many relevant aspects of the biology of this unicellular green alga have been reviewed by Pickett-Heaps (20). The mature, disk-shaped cell consists of two morphologically identical semicells, each with an elaborate set of symmetrical invaginations that divide the cell periphery into a series of lobes. During cell division, a septum forms across the narrow isthmus between the semicells. The septum then undergoes expansion and differentiation, which ultimately result in the formation of a new semicell. Synthesis of primary cell wall continues throughout this stage of development. Secondary wall synthesis commences at approximately the same time that growth of the semicell and synthesis of primary cell wall are completed (11). Sometime during or after synthesis of the secondary wall, the primary wall is shed. An amorphous layer, whose cleaving properties suggest a lipid composition (13), then forms exterior to the secondary wall.

In an earlier freeze-fracture study of the cell walls of *Micrasterias*, Kiermayer and Staehelin (13) found that the pattern of microfibril deposition was revealed by fractures through the fibrillar layer itself and could also be visualized in fractures through the amorphous layer, in which impressions of the bands of underlying fibrils can be seen. It is the highly ordered pattern of cellulosic fibril deposition in the secondary wall of *Micrasterias* that has allowed us to interpret the significance of the plasma membrane complexes observed in our freeze-fracture micrographs. Kiermayer and Dobberstein (6, 12) have shown in thin sections that these cells also possess characteristic heavily stained "flat vesicles" that appear to contain regular arrays of ~200 Å particles. The location of these vesicles in the cytoplasm suggests that they are formed by the Golgi complex and subsequently migrate to, and fuse with, the plasma membrane. The authors proposed that the rows of "particles" are thereby incorporated into the plasma membrane, where they give rise to the bands of parallel microfibrils of the secondary cell wall. The results presented here support and elaborate upon this hypothesis.

MATERIALS AND METHODS

Cultures of *Micrasterias denticulata* were obtained from the Algal Culture Collection, University of Indiana (Cat. No. LB558). Cells were grown in Waris medium MS (25) at 18°C on a 15/9-h, light-dark cycle. For each experiment, cells about halfway through the dark cycle were placed in fresh medium in continuous light. This treatment stimulated many cells to divide ~25 h later (9). Healthy, growing cells were then selected with a dissecting microscope and placed in a separate Petri dish containing growth medium buffered with 2 mM 2(*N*-morpholino)-ethane sulfonic acid adjusted to pH 6.0. Cells at the desired stage of development were then placed in another dish containing 1% glutaraldehyde in buffered medium and fixed for 20 min. Gold double-replica supports (Balzers High Vacuum Corp., Santa Ana, Calif.) were coated with a thin layer of yeast paste. Fixed cells were placed on one support and the second support was placed on top. This "sandwich" was plunged into liquid propane near its melting point and stored in liquid nitrogen. In some cases, cells were ultrarapidly frozen using a propane-jet device of the type described by Müller et al.[1] Samples were prepared as described above, with the following exceptions: cells were frozen directly in growth medium, without prior fixation; the gold supports used had been hollowed out, leaving a metal thickness of 0.005 in.; and the propane-jet device was used. Samples were fractured and replicated using a Balzers double-replica device in a Balzers BA 360 freeze-etch unit. Fracturing was done at −110°C. The yeast paste allowed recovery of large, intact replicas; these were cleaned in commercial bleach and 70% sulfuric acid at 60°C. Replicas were examined in a Jeol EM 100C or a Philips EM 300.

Most of the micrographs were mounted so that the direction of shadow is approximately from bottom to top. To critically assess the complementarity of the P- and E-face[2] images of fractured plasma membrane complexes, prints were made on transparent Kodak fine-grain positive film. The images were superimposed over one another using markers outside the complexes such as small blebs in the membrane to ensure proper alignment.

[1] Müller, M., N. Meister, and H. Moor. Freezing in a propane jet and its application in freeze-fracturing. Submitted for publication.

[2] The terminology of Branton et al. (1) is used to designate the fracture faces.

RESULTS

General Cell Wall Morphology

Freeze-fracture double replicas were obtained of cells of *Micrasterias denticulata* that had been frozen either during growth of the primary wall or during the period of secondary wall synthesis. A replica of two sister cells in which the young semicells have completed their gross morphogenesis and attained the same general shape as the older semicells is shown in Fig. 1. Some cracking and folding of the replica always occurred but was usually not extensive enough to hinder observation of the structural details.

The pattern of fibril deposition in secondary walls, revealed by fractures through the outer amorphous layer (Fig. 2) and through the fibrillar layer itself (Fig. 3), consists primarily of crisscrossing bands of up to 17 parallel fibrils. The impressions in the amorphous layer of underlying fibrils (Fig. 2) show the curvature of some bands and the occasional splitting off of individual fibrils. Fractures through the cellulose layer show that the size and shape of the fibrils vary. In general, the fibrils in the center of a band are large and appear planar, with a maximum width of about 28 nm, whereas those on the outside of the band are narrower and more rounded (Figs. 3 and 4). In spite of the varying width of the fibrils, the center-to-center spacing remains constant across the band, measuring 28 nm. In some cases, a distinct substructure consisting of fine longitudinal lines with a periodicity of ~5 nm is observed within each of the fibrils (Fig. 4).

Specialized Membrane Structures Observed during Secondary Wall Synthesis

Fractures through the plasma membrane of semicells engaged in secondary wall synthesis reveal the presence of elaborate complexes whose structure clearly correlates with the observed pattern of fibril deposition (Figs. 5 and 6). An area of the P-face of the plasma membrane of such a semicell is shown in Fig. 5. Several complexes, composed of varying numbers of subunits packed in a hexagonal array, can be seen. In several specimens, impressions of fibrils lying adjacent to the plasma membrane were observable as grooves on the P-face (Fig. 7) and ridges on the E-face (Fig. 8). Complexes could then be visualized at the termini of bands of fibrils, presumably reflecting the site of fibril elongation. The tight appression of the plasma membrane against the cell wall indicated by these micrographs could result from the formation of extracellular ice crystals or from the normal, high turgor pressure. The part of the complex fracturing with the P-face shown at high magnification in Fig. 6 consists of a precise hexagonal array of subunits called rosettes (after Mueller and Brown [15]). Each rosette appears to be composed of six particles packed tightly in a ring with an outside diameter of 22 nm and a central space of 7–8 nm. The individual particles measured about 8 nm in diameter. The center-to-center distance between adjacent rosettes is 33 nm. The repeat distance of the rows of rosettes, measured directly or calculated from the geometry of the hexagonal array, is 28.5 nm. These measurements remain constant throughout the complex. The largest complexes contain ~175 rosettes in ~16 rows and tend to be symmetrical. The rows of rosettes parallel to the direction of synthesis, when indicated by the impressions of fibrils, are longest in the center of the complex and taper toward the sides. As shown in Fig. 5, not all of the complexes are symmetrical, and some contain only a few short rows of rosettes. Fractures through the plasma membrane also reveal numerous particles that bear no obvious relationship to the rosettes or the fibrils (Figs. 7 and 8). These presumably participate in a wide range of activities associated with the plasma membrane other than fibril formation.

Use of the double-replica technique has allowed us to recover both complementary halves of some fractured complexes (Fig. 9). To carefully assess the complementarity of the E- and P-face images, prints made on transparent film were superimposed using markers outside of the complexes to ensure proper alignment. Part of the structure observed on the E-face consists of particles that seem to be complementary to the central hole of the P-face rosettes. Other particles are also evident. Most of these appear to arise from the fracturing of part of the rosette with the E-face, but a few E-face particles were found to lie between rosettes. Part of the periodicity observed on the E-face may also be the result of shallow depressions left behind when the rosettes were fractured away. It should be emphasized that the E-face image of the complex varied greatly. In some cases, virtually no particles were found, with only shallow depressions marking the location of the complex. When severe plastic deformation occurred during fracturing of some of the cells, a hexagonal array of


1

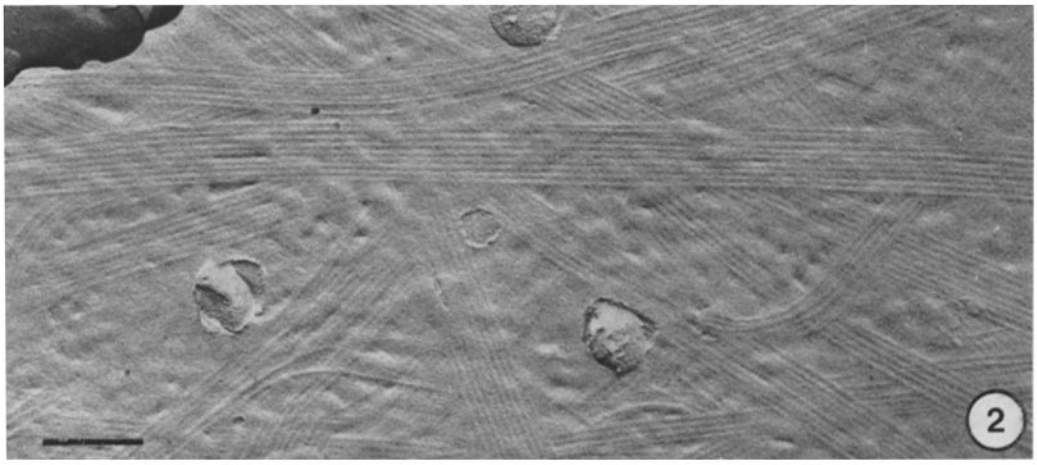
2

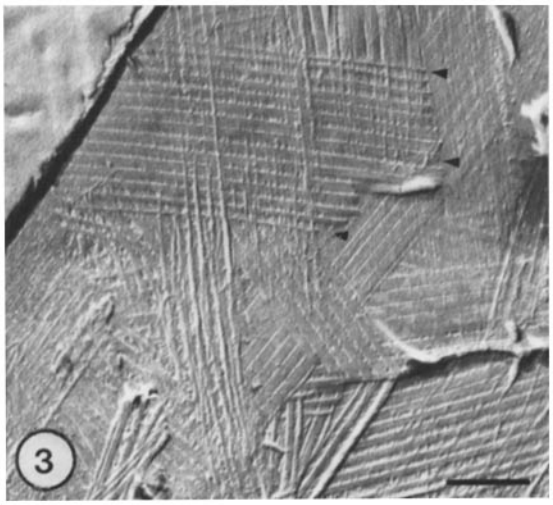
3

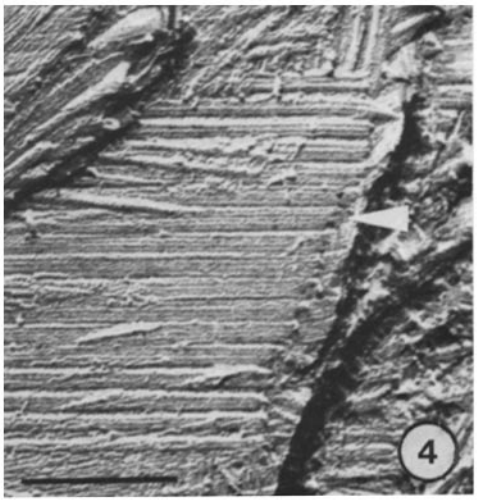
4

large particles was sometimes observed on the E-face. In such cases, the complementary P-face lacked clear rosettes, having instead severely deformed particles similar to those on the E-face.

Cells that were frozen with the propane jet occasionally fractured through the cytoplasm. Flat vesicles containing ordered arrays of rosettes on the P-face were found. In one case, both complementary halves were recovered (Fig. 10). In these micrographs, rosettes can be recognized on the P-face on both sides of the flat vesicles, whereas the E-face lacks observable structure. The sickle-shaped indentation of the plasma membrane with associated rosettes shown in Fig. 11 probably represents a site where a flat vesicle had just fused with the plasma membrane, thereby bringing the rosettes into position for synthesizing wall fibrils. A thin-section view of such a site is shown in Fig. 11 *a*.

Cells that had apparently completed primary wall growth and were involved in secondary wall synthesis also exhibited circular invaginations with a diameter of ~0.2 μm in their plasma membranes (Fig. 5). These structures are concave on the P-face and convex on the E-face. On the P-face, the invagination is usually particle rich relative to the surrounding membrane. The occurrence of the invaginations in a few semicells that had completed growth but did not show any indications of secondary wall formation suggests that these structures may begin to form just before the onset of secondary wall synthesis. All semicells with active complexes and secondary wall fibrils have these invaginations. Their distribution coincides with that of the putative slime secretory pores described by Kiermayer and Staehelin (13).

Specialized Membrane Structures Observed during Primary Wall Synthesis

The pattern of deposition of microfibrils during growth of the primary wall is markedly different from that during secondary wall formation. The microfibrils have an apparent diameter of 6–8 nm in freeze-fracture replicas and are randomly oriented (Fig. 12). Examination of the plasma membrane of semicells that were still expanding, and were, therefore, engaged in primary wall synthesis, revealed the presence of individual, randomly distributed rosettes rather than highly ordered complexes (Fig. 13). These rosettes have approximately the same dimensions as those found in the ordered complexes. The lack of microfibril impressions in the membrane prevented the visualization of rosettes in association with microfibrils. However, additional evidence for the role of these structures in primary cell wall synthesis comes from the observation that they are concentrated near the tips of the lobes (not shown),[3] where most of the wall deposition occurs (9). Vesicles containing a few single rosettes were detected in the cytoplasm of cells engaged in primary wall synthesis (Fig. 14).

DISCUSSION

Examination of freeze-fracture replicas of *Micrasterias denticulata* has revealed the presence of hexagonal arrays of particle rosettes in the plasma membrane of semicells engaged in the synthesis of the secondary wall. Our results suggest that these ordered complexes first appear at a point in the

[3] Brower and Giddings. Manuscript in preparation.

FIGURE 1 A freeze-fracture replica of two sister *Micrasterias* cells. The two young semicells (arrows) had just completed their expansion and gross morphological differentiation when the cells were frozen. As was typical, the younger semicells fractured mainly through the plasma membrane, whereas the older semicells fractured through the amorphous, lipidlike layer of the mature cell wall. Conventional freezing. Bar, 50 μm. × 480.

FIGURE 2 A fracture through the amorphous layer showing ridges corresponding to the fibrils of the underlying secondary cell wall. Conventional freezing. Bar, 0.5 μm. × 28,000.

FIGURE 3 A fracture through the fibrillar layer of the secondary cell wall. Note the crisscrossing bands of fibrils. The shift from broad to narrow fibrils and the constant spacing between them is particularly evident in the band indicated by arrowheads. Conventional freezing. Bar, 0.2 μm. × 55,000.

FIGURE 4 A band of fibrils at high magnification shows the change from flat, wide fibrils in the center to narrower, more rounded ones at the periphery. The substructure of the fibrils is also evident (arrowhead). Conventional freezing. Bar, 0.2 μm. × 103,000.

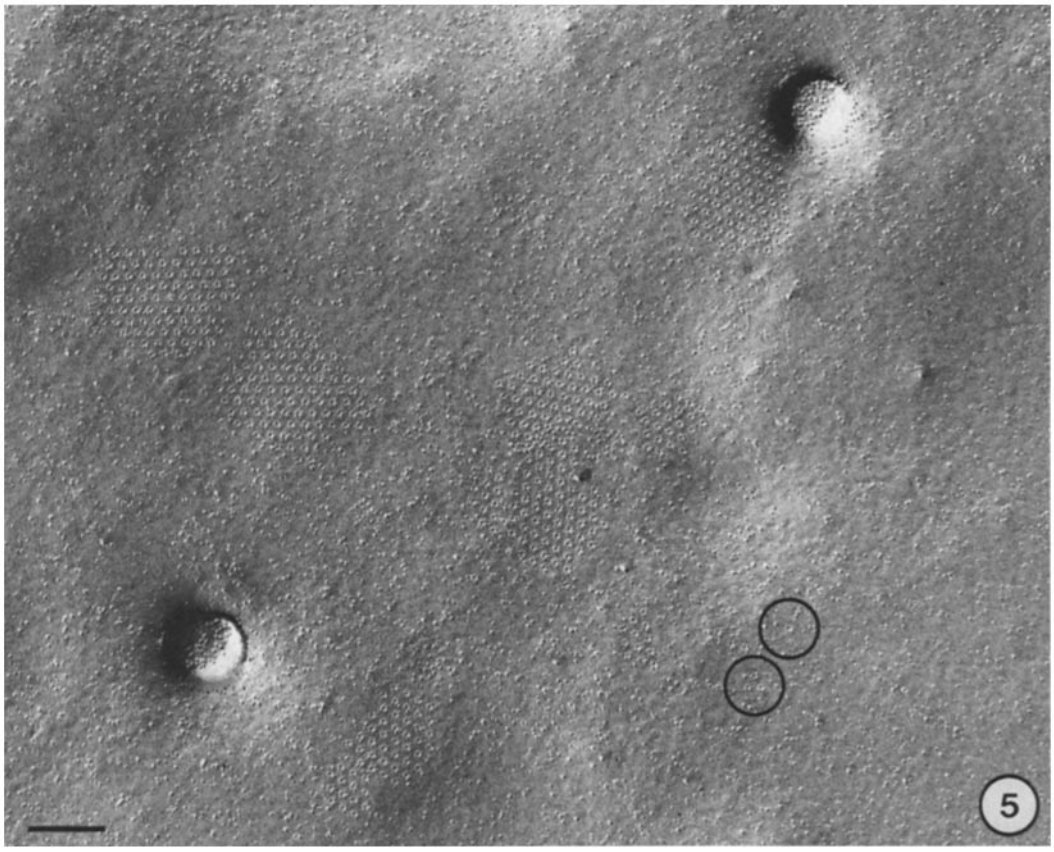
5

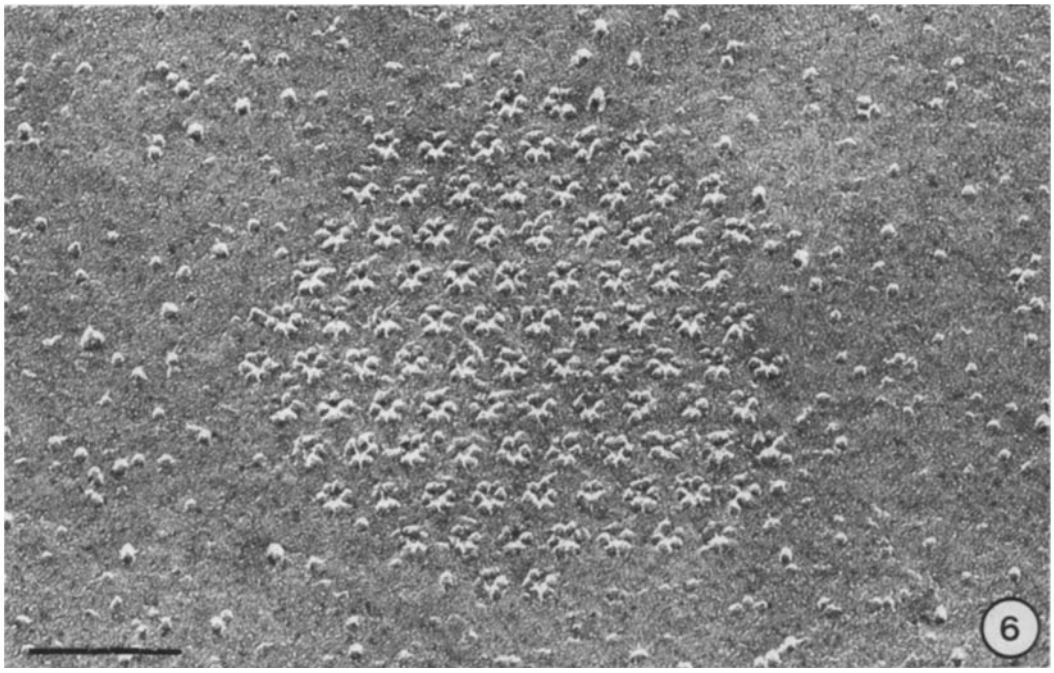
6

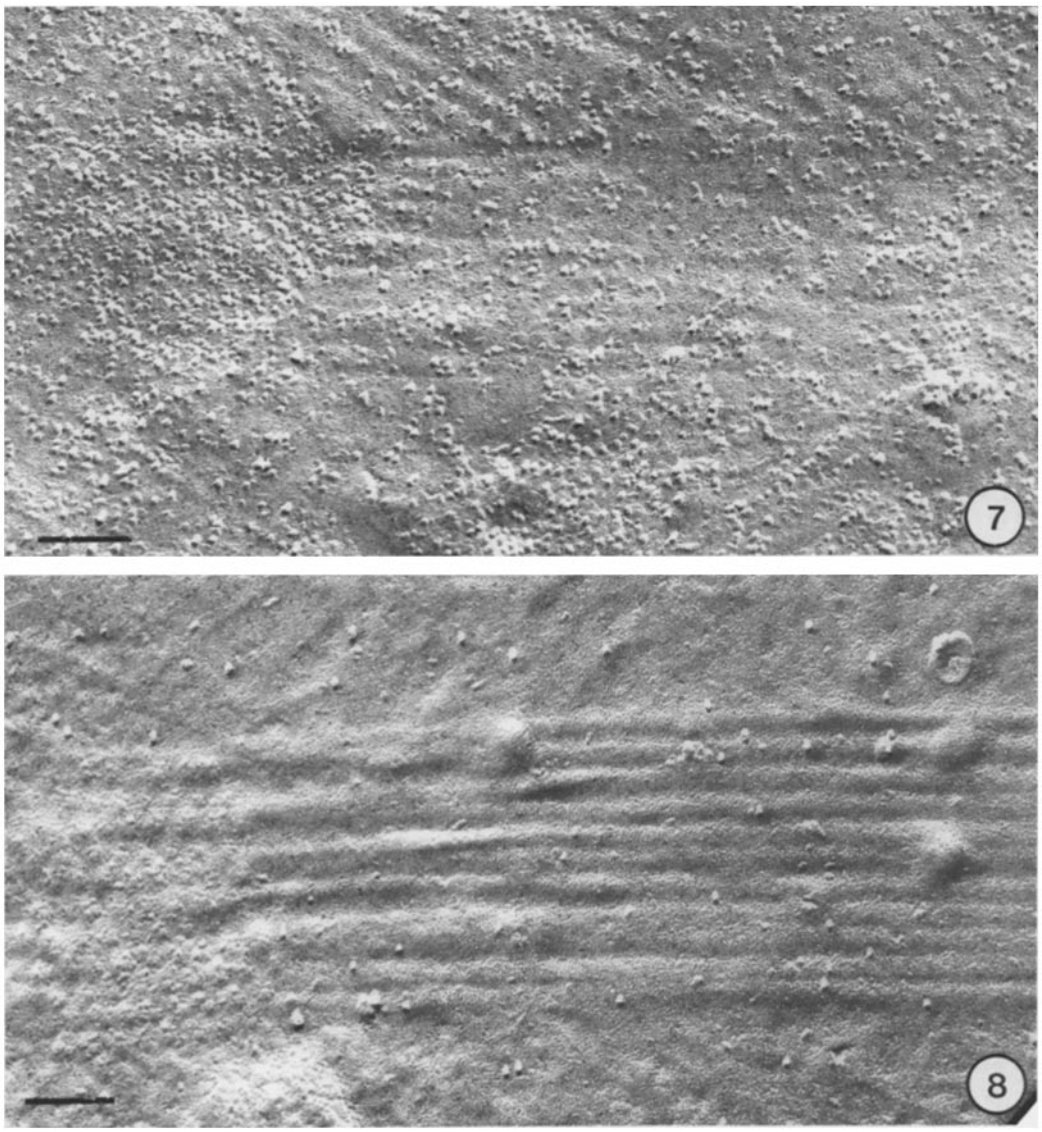

FIGURE 7 A complex on the P-face of the plasma membrane. In this case, grooves resulting from the appression of the plasma membrane against the fibrils can be seen aligned with rows of rosettes. Conventional freezing. Bar, 0.1 μm. × 118,000.

FIGURE 8 The E-face of a complex associated with ridges corresponding to newly synthesized fibrils. Conventional freezing. Bar, 0.1 μm. × 118,000.

FIGURE 5 The P-face of the plasma membrane of a semicell engaged in the synthesis of the secondary wall. Hexagonal arrays of rosettes of varying size and shape, as well as a few isolated rosettes (upper circle) can be observed. The lower circle indicates an array of three rosettes. The large circular indentations may correspond to forming slime secretion pore complexes. Propane-jet freezing. Bar, 0.2 μm. × 50,000.

FIGURE 6 The P-face of a complex consisting of a hexagonal array of rosettes at high magnification. The best-preserved rosettes are composed of six particles. Propane-jet freezing. Bar, 0.1 μm. × 200,000.

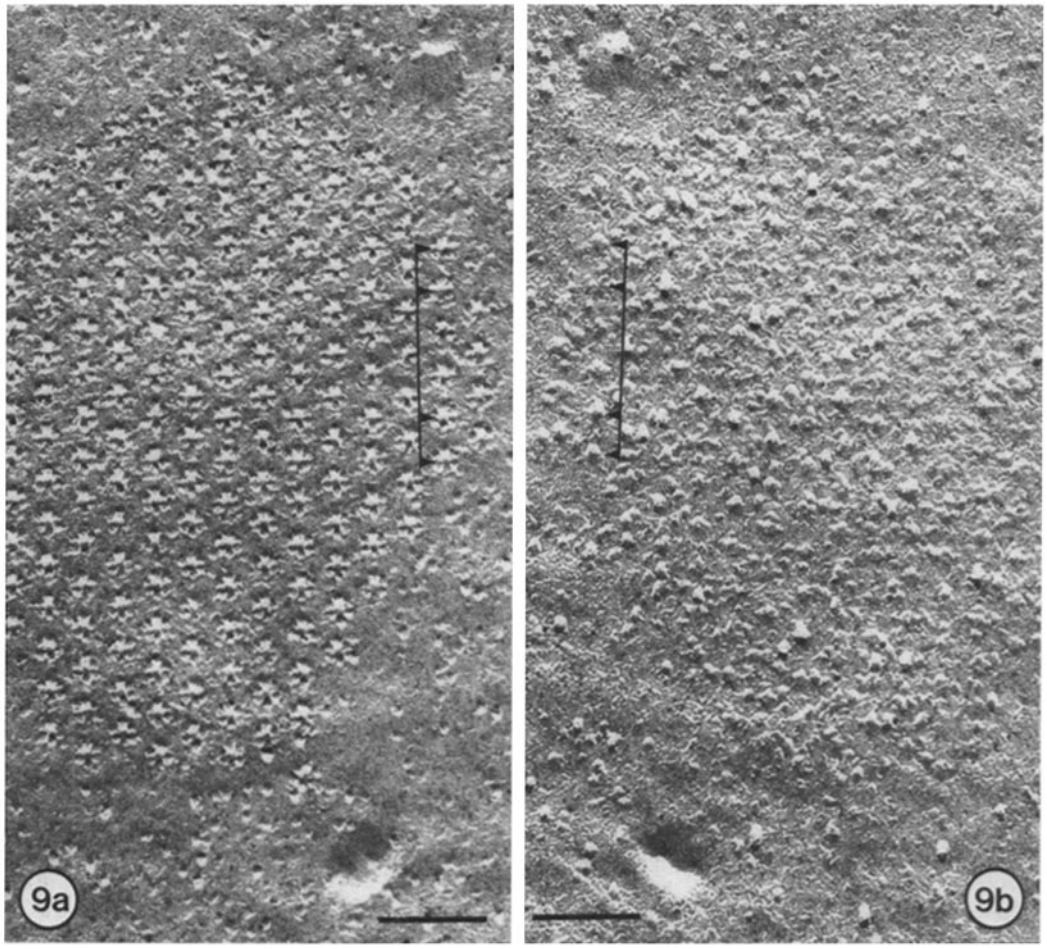

FIGURE 9 Complementary halves of a fractured complex. The P-face (*a*) shows the hexagonal array of rosettes. On the E-face (*b*), particles complementary to the central hole of the P-face rosettes are sometimes evident. The aligned arrowheads indicate exact complementary positions in the two micrographs. Propane-jet freezing. Bar, 0.1 μm. × 144,000.

cell cycle when the expansion and gross morphogenesis of the young semicell have stopped, and secondary wall synthesis normally is beginning. Direct evidence for the involvement of this complex in the synthesis of cellulosic fibrils comes from observation of the complexes at the tips of impressions of fibrils. Each row of rosettes appears to be associated with the formation of a fibril, the parallel rows of rosettes forming a band of parallel fibrils. This conclusion is also supported by the observation that the distance between fibrils is equal to the distance between rows of rosettes. Bands composed of varying numbers of fibrils can be accounted for by the presence of rosette arrays of varying size. In our specimens, complexes with as few as 3 and as many as 175 rosettes were observed.

The most significant aspect of this report is that the ordered pattern of fibril deposition in the secondary wall of *Micrasterias* can be shown to be derived from the structure of complexes located in the plasma membrane. Our results indicate that the widest fibrils, those in the center of a band, are formed by the longest rows of rosettes, those in the center of a complex, and shorter rows of rosettes give rise to narrower fibrils. The proportionality between the size of a fibril and the number of rosettes involved in its formation provides strong evidence that the rosette structure plays a significant role in the synthesis of cellulosic fibrils.

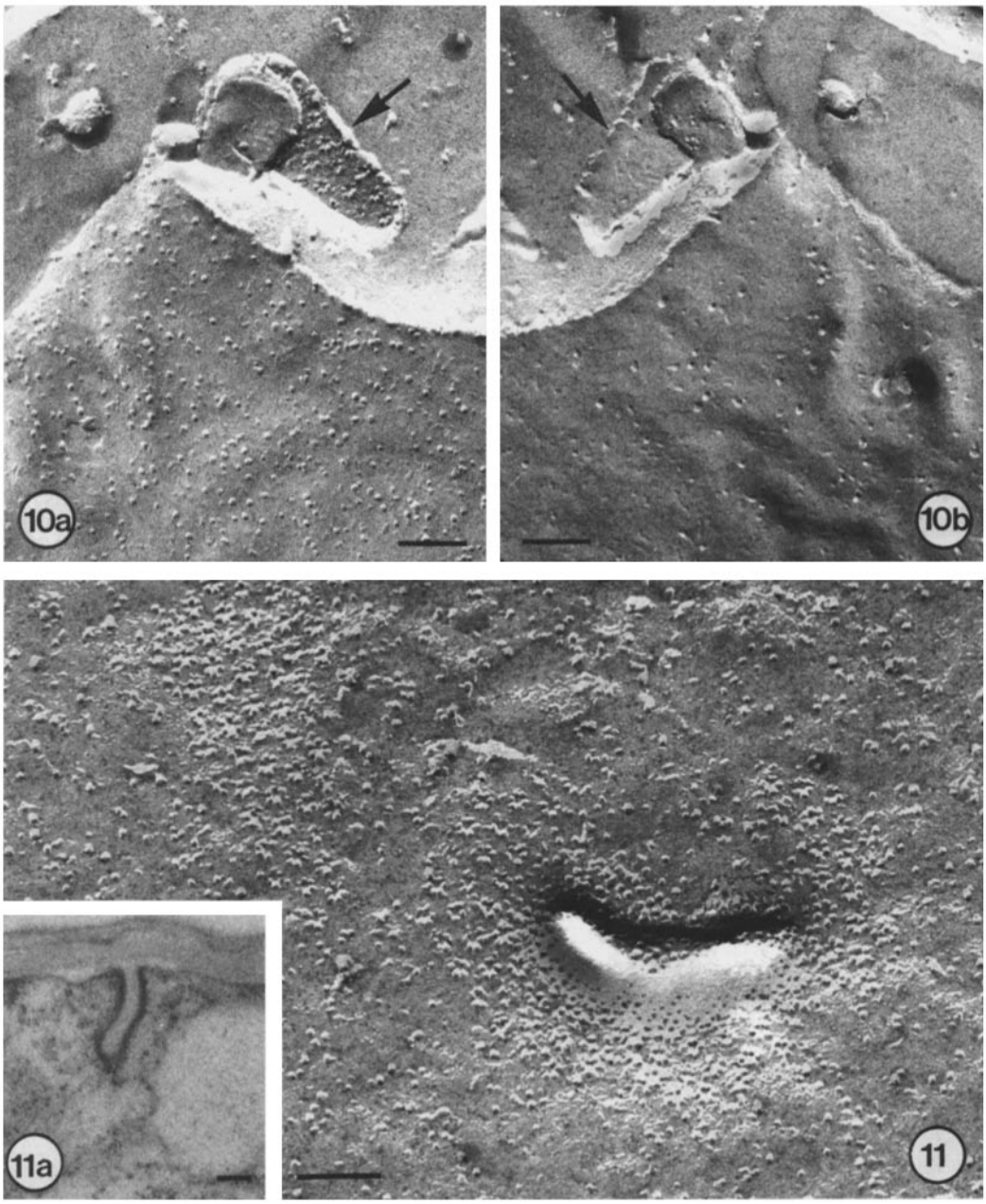

FIGURE 10 Complementary halves of a flat vesicle in the cytoplasm. (*a*) The P-face of the vesicle shows a hexagonal array of rosettes. (*b*) The E-face of the same vesicle lacks observable structure. Note that the P-face on both sides of the flat vesicle contains rosette units. The P-face of the plasma membrane is visible in *a*, and the complementary E-face is shown in *b*. Propane-jet freezing. Bar, 0.1 μm. × 96,000.

FIGURE 11 An area of the plasma membrane showing a crescent-shaped indentation with an ordered array of rosettes apparently emerging from it. Conventional freezing. Bar, 0.1 μm. × 117,000. (11 *a*) A thin-section view interpreted as showing a flat vesicle (heavily stained) which has fused with, and is being incorporated into, the plasma membrane (cf. Fig. 11). Bar, 0.1 μm. × 49,500.

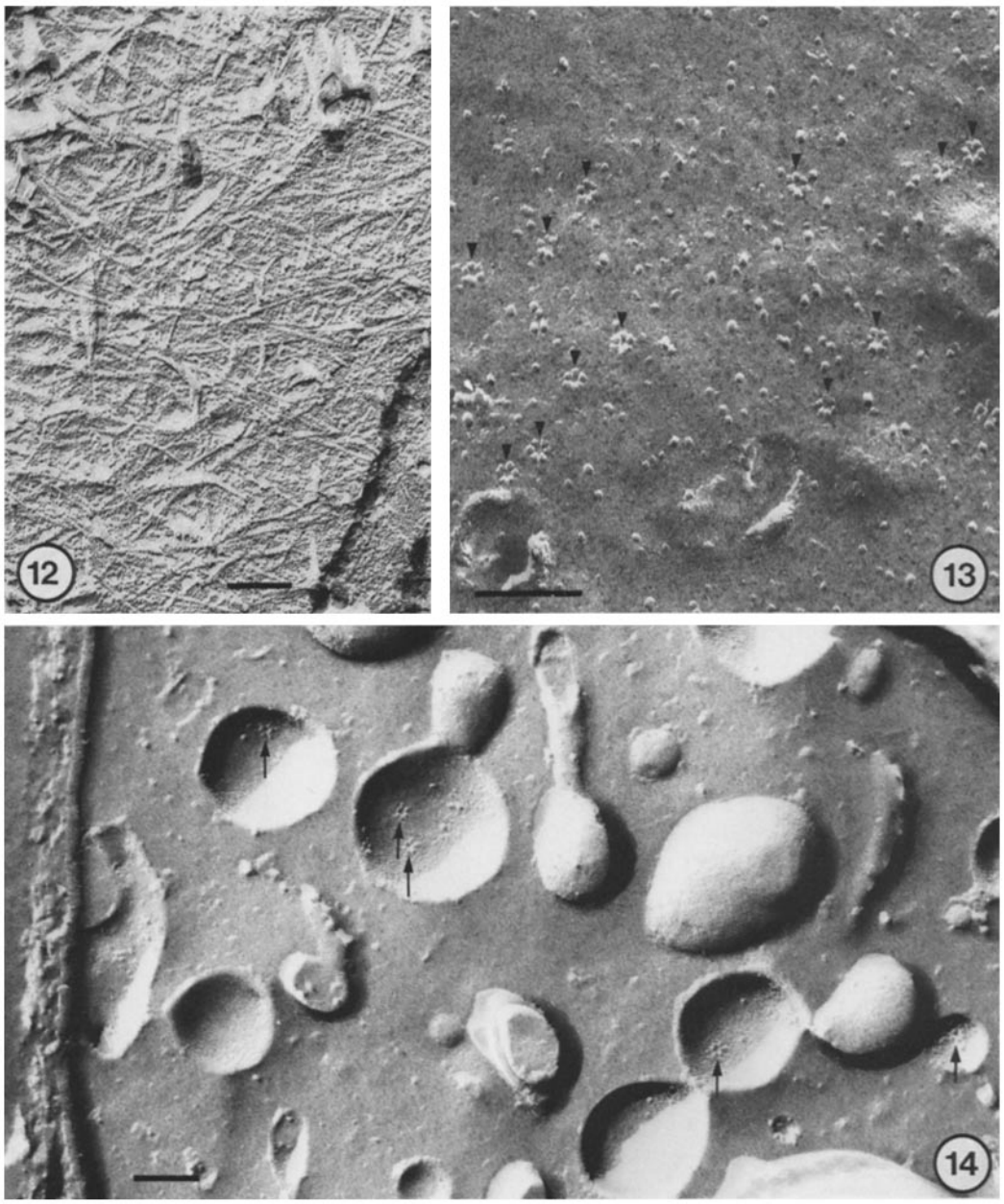

FIGURE 12 A fracture through a primary cell wall. Randomly oriented microfibrils with a diameter of 6–8 nm are observed. Conventional freezing. Bar, 0.1 μm. × 86,000.

FIGURE 13 The P-face of the plasma membrane of a semicell engaged in synthesis of the primary cell wall. Numerous single rosettes are found (arrowheads). Propane-jet freezing. Bar, 0.1 μm. × 150,000.

FIGURE 14 Vesicles in the cytoplasm of a semicell engaged in primary cell wall formation. The P-faces of many of the vesicles contain one or more single rosettes. Propane-jet freezing. Bar, 0.1 μm. × 81,000.

A schematic model illustrating this relationship is presented in Fig. 15. We suggest that each rosette accounts for one ~5-nm microfibril, and that these 5-nm microfibrils aggregate laterally to form the larger secondary wall fibrils. The observation of distinct longitudinal striations (periodicity ~5 nm) in the secondary wall fibrils (Fig. 4) is consistent with this model. The hexagonal packing of the 5-nm microfibrils suggested in the model is based on the observed shift from flat, wide fibrils in the center of a band to more rounded, narrower fibrils at the periphery, and on the number of rosettes involved in forming them. For example, the widest fibrils are believed to be the product of ~16 rosettes and show five striations on their surfaces. Packed three deep in a hexagonal manner, such a fibril could contain 16 microfibrils. If each microfibril measures ~5 nm in diameter, as is indicated in freeze-fracture, the model predicts a width of 30 nm. The observed maximum width is ~28.5 nm. A 5-nm microfibril could contain ~50 glucan chains. However, the extent to which substances other than cellulose-I contribute to the observed size is unknown. Nevertheless, it is of interest to consider the possibility that the 5-nm microfibrils that emanate from the individual rosettes could be structural equivalents of the "elementary fibrils" of Frey-Wyssling (7). The concept of "elementary fibrils" has been critically reviewed by Preston (21). In this context, the basic fibrillar unit could be redefined as the product of one rosette.

Analysis of complementary images of fractured complexes has proved useful, but not conclusive, in determining the complete structure of each rosette unit. Particles that fracture with the E-face and are complementary to the central hole of the rosettes are often, but not consistently, observed in the plasma membrane (Fig. 9). On the other hand, virtually no structure is detected on the E-face of cytoplasmic vesicles that contain the rosettes (Fig. 10). In view of the variability of the E-face images of the complexes, interpretation of these micro-

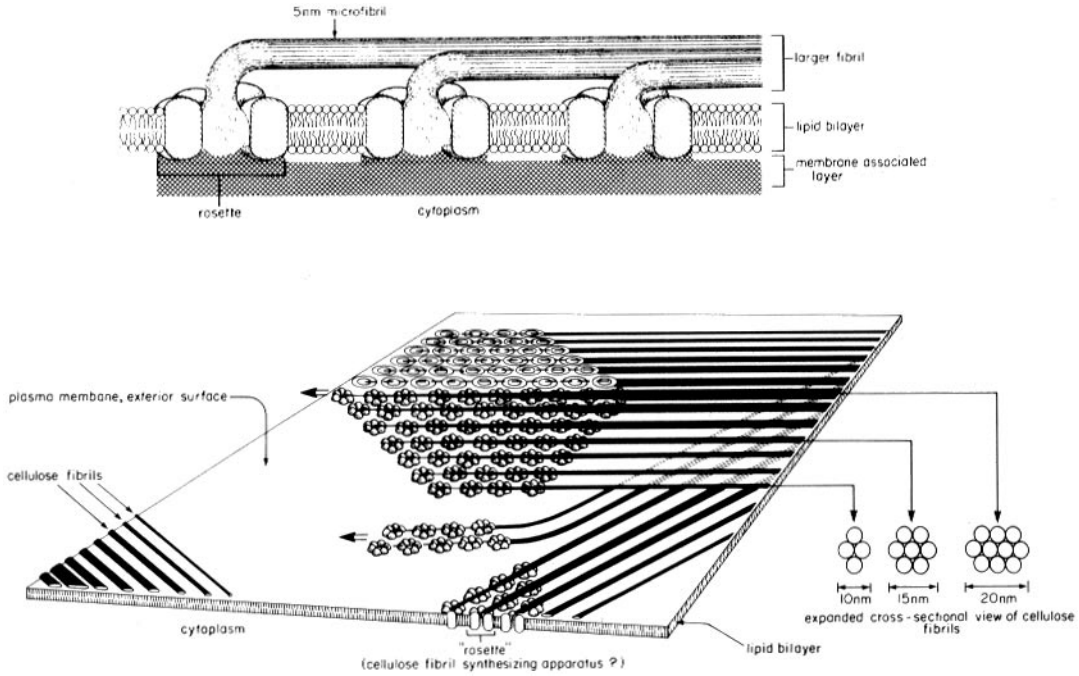

FIGURE 15 Model of cellulose fibril deposition during secondary wall formation in *Micrasterias*. Each rosette is believed to form one 5-nm microfibril. A row of rosettes forms a set of 5-nm microfibrils, which aggregate laterally to form the larger fibrils of the secondary wall. Above: side view. The stippled area in the center of a rosette represents the presumptive site of microfibril formation, although details of its structure, composition, and enzymatic activity remain unclear. The "membrane-associated layer" is based on the results of Kiermayer and Dobberstein (6, 12). This layer may serve to hold the rosettes together in the hexagonal array. Below: surface view with expanded cross-sectional view of cellulose fibrils.

graphs is difficult. They could indicate that forming microfibrils give rise to the E-face particles that are complementary to the central hole of the rosettes. No precise identity or enzymatic function can yet be ascribed to any of the observed particles on either fracture face.

Freeze-fracture and thin-section images such as those shown in Figs. 10 and 11 suggest that the complexes are first assembled into cytoplasmic vesicles and are subsequently incorporated into the plasma membrane by a process of vesicle fusion. Thus, our findings provide strong support for the hypothesis of cell wall formation of Kiermayer and Dobberstein (6, 12), which is based on their excellent thin-section studies of secondary wall formation in *Micrasterias*. These authors also produce evidence that the "flat vesicles" that contain the complexes are formed by the Golgi apparatus.

The pattern of deposition of the bands of fibrils suggests that the complexes move in the plane of the membrane. The mechanisms by which the complexes move and by which their orientation is controlled are unknown. Previous studies of thin sections of *Micrasterias* failed to detect any cytoplasmic structure whose position and orientation suggested a role in the guiding of microfibril synthesis (10). The complex may propel itself by the addition of monomers to the growing tips of the associated microfibrils. Our results suggest that the hexagonal arrays are fairly cohesive but occasionally break apart along an axis parallel to the direction of travel (Figs. 2 and 15). The thickened staining of the cytoplasmic leaflet of membranes containing the complexes that was reported by Kiermayer and Dobberstein (6, 12) could represent material that serves to keep the hexagonal array intact as it moves within the bilayer. The general direction taken by the complexes does appear to be random, the shape of the semicell having already been determined during primary wall growth.

The pattern of microfibril deposition during primary wall formation also seems to be random (Fig. 12). The relatively thin, 6–8-nm microfibrils appear to be the products of single rosettes, which can be visualized on the P-face of the plasma membrane of growing semicells (Fig. 13, and

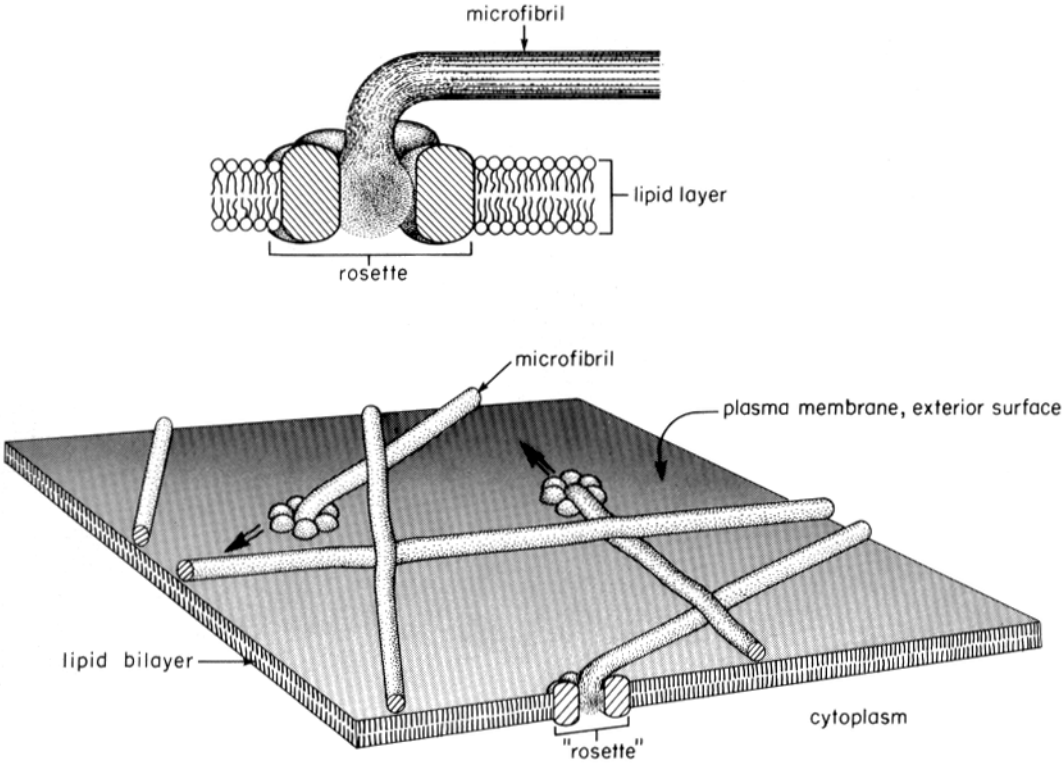

FIGURE 16 Model of microfibril deposition during primary wall formation in *Micrasterias*. Above: side view. Below: surface view. Single rosettes apparently give rise to randomly oriented microfibrils.

shown diagrammatically in Fig. 16). Vesicles containing small numbers of separate rosettes have been found in the cytoplasm of such cells, suggesting that the microfibril synthesizing units are assembled in cytoplasmic membranes and are incorporated into the plasma membrane by similar mechanisms during primary and secondary wall formation.

Intramembrane protein complexes, consisting, in part, of a rosette of six particles associated with the synthesis of cellulose microfibrils, have now been independently detected in a green alga, in fern protonemata (Wada and Staehelin, unpublished results), and in several higher plant cells (15, 16). Our report provides a correlation between the size of a given cellulose fibril and the number of rosette structures involved in its formation. All of the available evidence suggests that these structures represent morphological equivalents of plasma membrane-bound complexes of enzymes involved in the synthesis of cellulose fibrils in plants and green algae.

We would like to thank Dr. John Gilkey for expediting the construction of our propane-jet freezing device.

This work was supported by grant GM22912 from the Institute of General Medical Sciences to L. A. Staehelin, a Boettcher Foundation grant to D. L. Brower, and a University of Colorado Doctoral Fellowship to T. H. Giddings.

Received for publication 7 June 1979, and in revised form 11 September 1979.

REFERENCES

1. BRANTON, D., S. BULLIVANT, N. B. GILULA, M. J. KARNOVSKY, H. MOOR, K. MÜHLETHALER, D. H. NORTHCOTE, L. PACKER, B. SATIR, P. SATIR, V. SPETH, L. A. STAEHELIN, R. L. STEERE, and R. S. WEINSTEIN. 1975. Freeze-etching nomenclature. *Science (Wash. D. C.).* **190**:54–56.
2. BROWN, R. M., and D. MONTEZINOS. 1976. Cellulose microfibrils: visualization of biosynthetic and orienting complexes in association with the plasma membrane. *Proc. Natl. Acad. Sci. U. S. A.* **73**:143–147.
3. BROWN, R. M., and J. H. M. WILLISON. 1977. Golgi apparatus and plasma membrane involvement in secretion and cell surface deposition with special emphasis on cellulose biogenesis. *In* International Cell Biology 1976–1977. B. R. Brinkley and K. R. Porter, editors. The Rockefeller University Press, New York. 267–283.
4. BROWN, R. M., J. H. M. WILLISON, and C. L. RICHARDSON. 1976. Cellulose biosynthesis in *Acetobacter xylinum*: visualization of the site of synthesis and direct measurement of the *in vivo* process. *Proc. Natl. Acad. Sci. U. S. A.* **73**:4565–4569.
5. CHAFE, S. C., and A. B. WARDROP. 1970. Microfibril orientation in plant cell walls. *Planta (Berl.).* **92**:13–24.
6. DOBBERSTEIN, B., and O. KIERMAYER. 1972. Das Auftreten eines besonderen Typs von Golgivesikeln wahrend der Sekundärwandbildung von *Micrasterias denticulata* Bréb. *Protoplasma.* **75**:185–194.
7. FREY-WYSSLING, A. 1969. The ultrastructure and biogenesis of native cellulose. *Fortschr. Chem. Org. Naturst.* **27**:1–30.
8. GROUT, B. W. W. 1975. Cellulose microfibril deposition at the plasmalemma surface of regenerating tobacco mesophyll protoplasts: a deep etch study. *Planta (Berl.).* **23**:275–282.
9. KIERMAYER, O. 1964. Untersuchungen über die Morphogenese and Zellwandbildung bei *Micrasterias denticulata* Bréb. *Protoplasma.* **59**:76–132.
10. KIERMAYER, O. 1968. The distribution of microtubules in differentiating cells of *Micrasterias denticulata* Bréb. *Planta (Berl.).* **83**:223–236.
11. KIERMAYER, O. 1970. Causal aspects of cytomorphogenesis in *Micrasterias. Ann. N. Y. Acad. Sci.* **175**:686–701.
12. KIERMAYER, O., and B. DOBBERSTEIN. 1973. Membran komplexe dictyosomaler Herkunft als "Matrizen" für die extraplasmatische Synthese und Orientierung von Mikrofibrillen. *Protoplasma.* **77**:437–451.
13. KIERMAYER, O., and L. A. STAEHELIN. 1972. Feinstruktur von Zellwand und Plasmamembran bei *Micrasterias denticulata* Bréb. nach Gefrierätzung. *Protoplasma.* **74**:227–237.
14. MONTEZINOS, D., and R. M. BROWN, JR. 1976. Surface architecture of the plant cell: biogenesis of the cell wall, with special emphasis on the role of the plasma membrane in cellulose biosynthesis. *J. Supramol. Struct.* **5**:277–290.
15. MUELLER, S. C., and R. M. BROWN, JR. 1978. Characterization of the presumptive cellulose synthesizing system in corn root cells. *J. Cell Biol.* **79**(2, Pt. 2):237 *a* (Abstr.).
16. MUELLER, S. C., and R. M. BROWN, JR. 1980. Evidence for an intramembrane component associated with a cellulose microfibril synthesizing complex in higher plants. *J. Cell Biol.* **84**:315–326.
17. MUELLER, S. C., R. M. BROWN, JR., and T. K. SCOTT. 1976. Cellulose microfibrils: nascent stages of synthesis in a higher plant cell. *Science (Wash. D. C.).* **194**:949–951.
18. NORTHCOTE, D. H., and D. R. LEWIS. 1968. Freeze-etched surfaces of membranes and organelles in the cells of pea root tips. *J. Cell Sci.* **3**: 199–206.
19. PENG, H. B., and L. F. JAFFE. 1976. Cell wall formation in *Pelvetia* embryos. A freeze-fracture study. *Planta (Berl.).* **133**:57–71.
20. PICKETT-HEAPS, J. D. 1975. Green Algae: Structure, Reproduction and Evolution in Selected Genera. Sinauer Associates Inc., Sunderland, Mass.
21. PRESTON, R. D. 1974. The Physical Biology of Plant Cell Walls. Halsted Press, New York.
22. ROBENEK, H., and E. PEVELING. 1977. Ultrastructure of the cell wall regeneration of isolated protoplasts of *Skimmia japonica* Thunb. *Planta (Berl.).* **136**:135–145.
23. ROBINSON, D. G., and R. D. PRESTON. 1971. Fine structure of swarmers of *Cladophora* and *Chaetomorpha*. I. The plasmalemma and Golgi apparatus in naked swarmers. *J. Cell Sci.* **9**:581–601.
24. ROBINSON, D. G., and R. D. PRESTON. 1972. Plasmalemma structure in relation to microfibril biosynthesis in *Oocystis. Planta (Berl.).* **104**:234–246.
25. WARIS, H. 1953. The significance for algae of chelating substances in the nutrient solutions. *Physiol. Plant.* **6**:538–543.
26. WILLISON, J. H. M. 1976. An examination of the relationship between freeze-fractured plasmalemma and cell-wall microfibrils. *Protoplasma.* **88**:187–200.
27. WILLISON, J. H. M., and R. M. BROWN, JR. 1977. An examination of the developing cotton fiber: wall and plasmalemma. *Protoplasma.* **92**: 21–41.
28. WILLISON, J. H. M., and R. M. BROWN, JR. 1978. Cell wall structure and deposition in *Glaucocystis. J. Cell Biol.* **77**:103–119.
29. WILLISON, J. H. M., and E. C. COCKING. 1972. The production of microfibrils at the surface of isolated tomato-fruit protoplasts. *Protoplasma.* **75**:397–403.
30. WILLISON, J. H. M., and E. C. COCKING. 1975. Microfibril synthesis at the surfaces of isolated tobacco mesophyll protoplasts, a freeze-etch study. *Protoplasma.* **84**:147–159.
31. ZAAR, K. 1977. The biogenesis of cellulose by *Acetobacter xylinum. Cytobiologie.* **16**:1–15.
32. ZAAR, K. 1979. Visualization of pores (export sites) correlated with cellulose production in the envelope of the gram-negative bacterium *Acetobacter xylinum. J. Cell Biol.* **80**:773–777.